International Journal of Mechanical and Production
Engineering Research and Development (IJMPERD)
ISSN(P): 2249–6890; ISSN(E): 2249–8001
Vol. 9, Issue 4, Aug 2019, 1311–1324

CHARACTERIZATION OF STRUCTURAL PROPERTIES AND HARDEN ENHANCEMENT OF AL-CU-N BY THIN FILM COATING

R. HARIHARAN[1*] & R. RAJA[2]

*[1]Research Scholar, Assistant professor, Department of Mechanical Engineering,
Bharath Institute of Higher Education and Research, Chennai, Tamil Nadu, India*

*[2]Professor, Department of Mechanical Engineering, Bharath Institute of Higher
Education and Research, Chennai, Tamil Nadu, India*

ABSTRACT

Two series of Al-Cu-N films containing Cu were grown by DC / RF magnetron sputtering of two elemental targets in an Ar / N & sub2; Gas mixture deposited by biasing a high-speed steel substrate. The effects of Cu content and deposition conditions were investigated with respect to the microstructure, morphology and mechanical properties of the films. The structure and mechanical properties of these films were dependent on the copper concentration. X-ray diffraction analysis and high-resolution and standard transmission microscopy analyzes show that the particle size in the film decreases with increasing copper content, but the sign of the copper-cutting content has not been determined. The micro hardness and adhesion of the coating/substrate were analyzed with a micro hardness tester and a scratch test.

KEYWORDS: DC/RF Magnetron Sputtering, Ar-N2 Gas Mixture & X-ray Diffraction

Received: May 13, 2019; **Accepted:** Jun 03, 2019; **Published:** Aug 01, 2019; **Paper Id.:** IJMPERDAUG2019136

Original Article

INTRODUCTION

Aluminum nitride (AlN) may be a broadband compound (6.2 eV) [1-3] III-V, attracting scientific attention because of its exotic nature. personal skinny films having a hexangular wurtzite crystal structure square measure utilized in varied applications like exhausting optical coatings, wear-resistant electronics, warm temperature, chemical, and thermal stability. With its high thermal conduction (180 Wm-1 K-1), wonderful piezo effect, high electrical electric resistance (ρ = 109-1011 Ω m) and quick sound rate, AlN could be a promising material to be used in optoelectronic devices, Surface acoustic thin-film sensors and resonators. A thermally semiconducting AlN film having an acceptable material constant is taken into account for semiconductor MOS applications. AlN films square measure is used for optical applications in corrosive and high-temperature environments. The thin film quality of AlN needs a high purity source associate degreed an oxygen-free surrounding for deposition thanks to the reactivity of the metal. Historically, AlN films square measure deposited by varied techniques, ideally chemical vapor deposition (CVD) or molecular beam growing (MBE), periodic optical maser deposition (PLD) and electron sputtering. Recently, several reports on the low-temperature deposition of high-quality AlN films victimization physical vapor deposition (PVD) techniques unit accessible at intervals. The PVD technique, DC electron tube sputtering is at the foremost of typical deposition technique. Among these, sputtering has edges over different conventionally used high-temperature technologies because of its simplicity, its agent, its low worth, and its ability to supply good quality films at all-time low temperature and have desired properties. The properties of the ready film depend upon the parameters and process methodology and square measure easier to regulate

within the PVD method. During this study, AlN films square measure deposited on semiconductor and glass substrates by DC vacuum tube sputtering to realize the required properties, we tend to observe the result of power on section, structure and film formation on Si and glass substrates. All deposits square measure created by maintaining a relentless gas magnitude relation, deposition temperature, and base pressure. Thin films square measure characterized by diffraction (XRD), atomic force research (AFM) and spectroscopical ellipsometry. The optical properties of the film square measure analyzed victimization associate degree ultraviolet-visible mass spectrometer and Fourier remodels infrared chemical analysis (FTIR). The optical properties of skinny films are studied by varied analytical and numerical strategies. In these strategies, coefficient and coefficient of reflection information were accustomed to calculate optical constants of thin films like ratio n (λ), extinction constant k (λ) and film thickness D.

Structural and Optical Properties of Aluminum Nitride Thin Films Deposited by Pulsed DC Magnetron Sputtering, R. K. Choudhary, 1 P. Mishra, 1 A. Biswas, 2 and A. C. Bidaye1, Thin films of aluminum nitride were deposited on Si (100) substrates by periodic sputtering of a reactive vacuum DC tube (asymmetric bipolar) under an alternating flow of chemical elements in an inert gas mixture and chemical elements. The deposited films were characterized by methods of slide dip (GIXRD), atomic force magnifier (AFM), spectroscopic ellipsometry and X-ray diffraction on secondary ion mass spectrometry (SIMS). The results of GIXRD show the (100) reflection of wurtzite AlN, but AFM micrographs have a very fine-grained microstructure with an average roughness of 6-8 nm. Ellipsometry spectroscopy showed the film's bandgap and ratios ranging from 5.0 to 5.48 energy units and 1.58 to 1.84, respectively. SIMS measurements indicated the presence of oxygen in the film.

The properties of thin layers of copper nitride deposited by a pulsed discharge with a hollow cathode, Khaled Hussein Metvali, Hassan Saudi Ali and Farouk Fahmi El-Akshar Copper nitride (Cu 3 N) on a glass substrate with a hollow cathode of pulsed glass) Applying a thin film a voltage of 4 kV and a pressure of gaseous nitrogen of 10 -2 Torr. The thin-film structure was identified by X-ray diffraction (XRD). X-ray diffraction measurements showed that this thin film was nano crystalline and showed orientation in the (111) Cu 3 N 5 phase. The grain size of the nanocrystal films ranged from 41 nm to 80 nm. The bandgap was measured using a UV-Vis-NIR spectrophotometer and a contact equation. Increasing the number of taps from 20 to 80 taps increased the optical bandgap of the film from 2.55 eV to 2.25 eV. Surface morphology was examined using a Scanning Electron Microscope (SEM). SEM image shows that the film has filled particles with the morphology of a faceted surface.

Reactive sputtering of thin films of aluminum nitride (002) for piezoelectric applications in the production of aluminum nitride films (AlN) with extremely high axis for piezoelectric applications, Abis Iqbal, Faisal Mohd-Yasin, Summarize Recipe. This usually describes the role of spray parameters. The data is compared to an analysis of approximately 80 journal articles where this film was sprayed onto the substrate material, process and equipment. This review is a good place to familiarize yourself with the current analysis of reactive sputtering of thin AlN (002) films and a list of developments for piezoelectric applications such as energy collectors.

The impact of nitrogen plasma on a copper thin film deposited by DC magnetron sputtering, A. Hojabri, N. Haghighian, K. Yasserian, M. Ghoranneviss, Copper nitride (Cu 3 N) thin film surface units are obtained under the influence of copper thin films on nitrogen plasma under various conditions. Copper thin-film area units deposited on Si substrates under certain conditions suggest that DC magnetron sputtered area units are next exposed to low-temperature nitrogen plasma. The influence of nitrogen plasma on the structure, morphology, hardness, electrical and optical properties of copper thin films have been studied for many periods. The x-ray diffraction pattern confirms that the increase in time

annihilates the copper portion, thus reducing the roughness of the film while the square of the copper nitride phase is detected.

EXPERIMENTAL PROCEDURE

Ultrasonic amplification may be a modification (sometimes for traditional water treatment procedures) adapted to a soluble solution (most often between 20 and 400 kHz) for treatment and washing with ultrasound. Ultrasound is used in freshwater, but the use of soluble substances adapted to the washed factors, and thus the rational elimination of waste, improves exposure. The improvement usually takes 3 to 6 minutes, but some claims may exceed 20 minutes. Supersonic motion (cavitation) contributes to the reaction to the impact on activity. Normal water will not be strong at all. The cleaning arrangement contains fixings intended to make ultrasonic cleaning more successful. For instance, lessening of surface strain expands cavitation levels, so the arrangement contains a decent wetting specialist (surfactant). Watery cleaning arrangements contain cleansers, wetting operators and different parts, and impact the cleaning procedure. Revise piece of the arrangement is extremely needy upon the thing cleaned. Arrangements are for the most part utilized warm, at around 50– 65 °C (122– 149 °F), in any case, in therapeutic applications it is by and large acknowledged that cleaning ought to be at temperatures underneath 45 °C (113 °F) to forestall protein coagulation.

Grinders, often abbreviated as grinders, are a variety of power tools or machines that are used for grinding, which may be various machining processes using on-wheels for cutters. The presence of rough, coarse abrasive grains on the surface of the grinding wheel can result in small chips during machining up to a small twist. Polishing is finishing procedures for smoothing a workpiece's surface utilizing AN abrasive and a work wheel or an animal skin strop. Sharpening alludes to forms that utilization AN abrasive that's stuck to the work wheel, whereas buffing utilizes a free grating connected to the work wheel. Cleansing may be a lot of forceful methods whereas buffing is a smaller amount cruel, that prompts a power tool, brighter finish. A typical misinterpretation is that a cleansed surface includes a mirror splendid complete, however, most mirror sensible completions square measure were buffed. Cleansing is often accustomed to improve the presence of an issue, avert pollution of instruments, evacuate oxidization, build AN intelligent surface, or avoid erosion in channels. In metallography and science, cleansing is employed to form tier, imperfection-free surface for AN examination of a metal's microstructure underneath a magnifying instrument. Silicon-based cleansing cushions or a jewelry arrangement are often used as a part of the cleansing procedure. Cleaning stainless-steel will likewise build its sterile benefits. The expulsion of oxidization (discolor) from metal articles is refined utilizing a metal clean or stain remover; this is likewise called cleaning. To anticipate to encourage undesirable oxidization, cleaned metal surfaces might be covered with wax, oil, or polish. This is of specific worry for copper compound items, for example, metal and bronze the condition of the present material makes sense of what sort of grinding will be associated. The better abrasives leave persistently better lines that are not discernible to the uncovered eye. To achieve a #8 Finish (Mirror) it requires cleaning and buffing blends, cleaning wrangles speed cleaning machines or other machine mechanical assemblies that can be used for cleaning, like an electrical bore. Oils like wax and kerosene may be used as lubing up and cooling media in the midst of these exercises, though some cleaning materials are especially proposed to be used dry.

(a) (b)

Figure 1: (a) Before Polishing (b) After Polishing

(a) (b)

Figure 2: Substrate (a) Before Coating (b) After Coating

Figure 3: Machine Setup

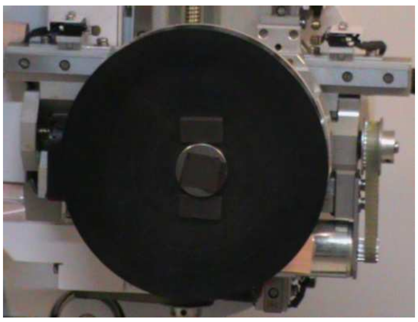

Figure 4: During Processing

Coating by RF/DC Magnetron Sputtering

Table 1: Coating Parameters by RF/DC Magnetron Sputtering

PARAMETERS	100°C	200°C	300°C
Chamber base pressure	4xm.bar	4xm.bar	4xm.bar
Deposition pressure	2xm.bar	2xm.bar	2xm.bar
Target to substrate distance	60 mm	60 mm	60 mm
Argon flow rate	15sccm	15sccm	15sccm
Nitrogen flow rate	3sccm	3sccm	3sccm
Al (DC)	100 w	100 w	100 w
Cu (RF)	100 w	100 w	100 w
Substrate temp	100°c	200°c	300°c
Cu interlayer	5 min	5 min	

WORKING METHODOLGY

X-Ray Diffraction

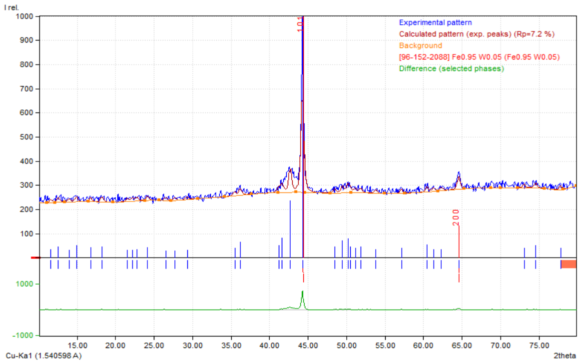

Figure 5: Xrd Patterns of Al-Cu-N Coated At 100^{0}c

Figure 5 shows the x-ray diffraction diagrams of M2 steel coated with AlCuN at 100^0 c, the diffraction peaks from the substrate there are main peaks of cubic AlCuN a significant peak at 42. This is from 0 to 42 at this point the highest peak is shown and then normal small curves were appeared at a range of (101) and (200) this whole diffraction. X-ray diffraction of the 100˚c of the different parameters of the data range 9.942˚–79.813˚ and the wave length is 1.540598A˚. Full width at half maximum (FWHM) at 2θ is (-0.11˚) and the full width at half maximum (FWHM) is 0.4326. Rp is calculated pattern Rp=7.2% and (200) simple cubic present at 45˚c can have a multiple-atom basic. A copper phase appears in the pattern (Cu0.78 In2.078 Se3.6).

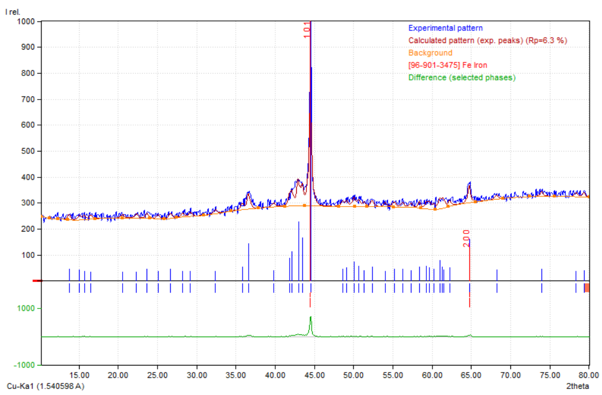

Figure 6: Xrd Patterns of Al-Cu-N Coated at 200^{0}c

Figure 6 shows the x-ray diffraction diagrams of M2 steel coated with AlCuN at 200^{o} c, the diffraction peaks from the substrate there are main peaks of cubic AlCuN a significant peak at 44. This is from 0 to 44 at this point the highest peak is shown and then normal small curves have appeared at a range of (101) and (200) of this whole diffraction. X-ray diffraction of the 200˚c of the different parameters of the data range 10.132˚-80.003˚ and the wavelength is 1.540598A˚. The full width at half maximum (FWHM) at 2θ is (0.08˚) and the full width at half maximum (FWHM) is 0.4326. Rp is calculated pattern Rp = 6.3%. Copper and aluminium phases appear in the pattern (Cu0.875Ga0.115) and (Al0.5 Ga0.5) Co).

Figure 7 shows the x-ray diffraction diagrams of M2 steel coated with AlCuN at 300^{0}c, the diffraction peaks from the substrate there are main peaks of cubic AlCuN a significant peak at 44. This is from 0 to 44 at this point the highest peak is shown and then normal small curves appear at a range of (101) and (200) of this whole diffraction. X-ray diffraction of the 200˚c of the different parameters of the data range 10.052˚-79.923˚ and the wavelength is 1.540598A˚. Full width at half maximum (FWHM) at 2θ is (0.08˚) and the full width at half maximum (FWHM) is 0.4326. Rp is calculated pattern Rp = 7.7%. Copper phases appears in the pattern (Ag0.04 Cu3.96) (Cu0.951 Zn0.049). The physical properties of the cal.density is 6.82200 g/cm3.

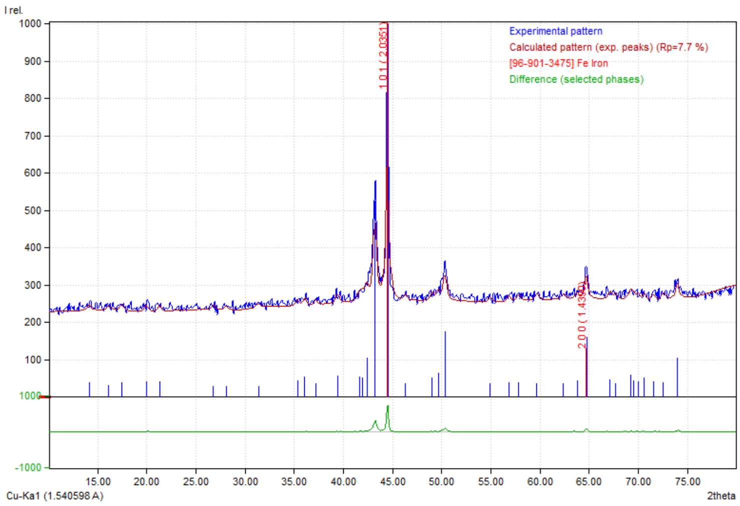

Figure 7: Xrd Patterns of Al-Cu-N Coated at 300^{0}c

Atomic Force Microscopy (AFM)

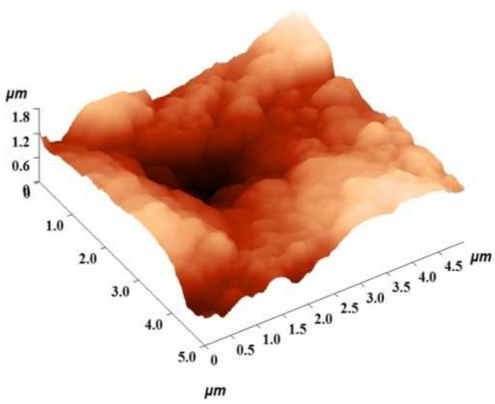

Figure 8: 5µm × 5µm 3D Image of Coated Sample at 100°C

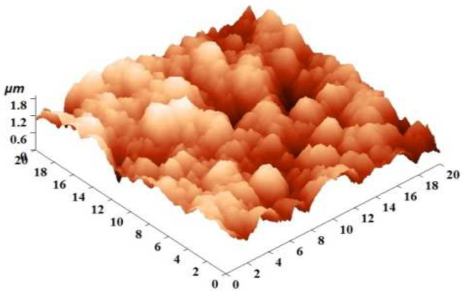

Figure 9: 20µm × 20µm 3D Image of Coated Sample at 100°C

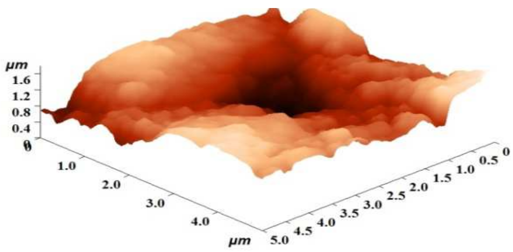

Figure 10: 5µm × 5µm 3D Image of Coated Sample at 200°C

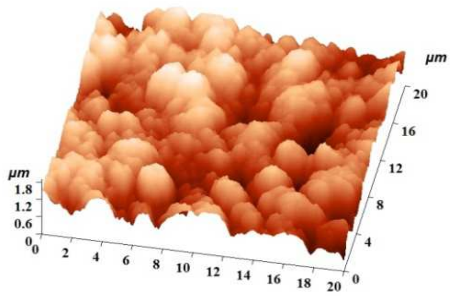

Figure 11: 20µm × 20µm 3D Image of Coated Sample at 200°C

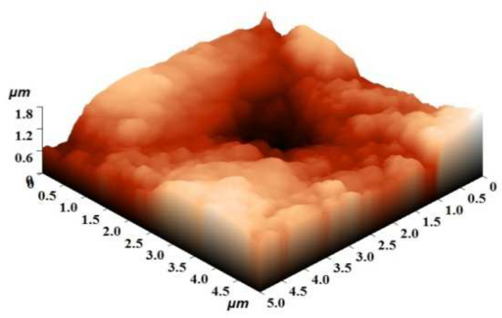

Figure 12: 5µm × 5µm 3D Image of Coated Sample at 300°C

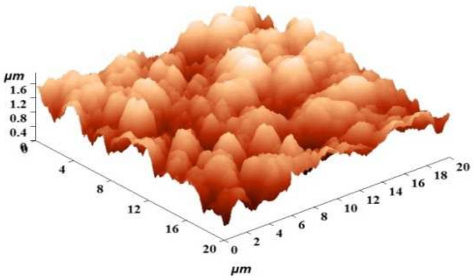

Figure 13: 20µm × 20µm 3D Image of Coated Sample at 300°C

Table 2: 20µm × 20µm Roughness Parameters

20µm × 20µm Roughness Parameters	
Average Roughness, Sa	232.965 nm
Root Mean Square, Sq	292.862 nm
Surface skewness, Ssk	-0.491592
Coefficient of kurtosis, Ska	0.306814
Entropy	13.2509
Redundance	-0.215247

Table 3: 5µm × 5µm Roughness Parameters

5µm × 5µm Roughness Parameters	
Average Roughness, Sa	245.58 nm
Root Mean Square, Sq	316.428 nm
Surface skewness, Ssk	-0.657241
Coefficient of kurtosis, Ska	0.394882
Entropy	13.276
Redundance	-0.226781

Atomic force microscopy (AFM) is one of the portrayal strategies generally utilized for the surface investigation. This method is extremely appealing for surface imaging of different materials. The surface morphology of the movies was researched with AFM in the non-contact mode utilizing a silicon nitride cantilever. The nuclear power pictures demonstrate the adjustment in the morphology of the film with the adjustment in the temperature. The Al-Cu-N film saved at 100 ^{o} c & 200 ^{o}c shows harsh sporadic structure, while, the AFM picture Al-Cu-N film saved at 400 ^{o}c shows lesser surface highlights, joined with an expansion in the harshness (Sa) of the film (i.e. 232.965 nm) Sq (292.862 nm) at 20µm × 20µm. Surface projections at standard interims of a similar size and expanded unpleasantness are seen in Al-Cu-N films kept at 200 ^{o} c while test covered at 400 ^{o} c had projections at unpredictable intervals. By contrasting the pictures we can state that as the temperature of the coating increases roughness and surface irregularities were increased.

The roughness estimations of all temperature entropy are maintained at 13.2509. At 400^{o}C example, it is 245.58 nm (5µm × 5µm). By looking at all the qualities at various temperatures we observed that the roughness estimation of the 400^{o}C example is higher than the 100^{o}C &200^{o}C sample. By this, we can affirm that the unpleasantness esteem will increment as the temperature increments.

Cross-sectional pictures of Al-Cu-N coatings saved under various temperatures appeared in figure 8 to 13. From figure 8 & 9, we watched cracks apart at 10µm scale. Under different amplifications and scales, we observed unpredictable structures on the 100^{o}C sample. For tests covered at 200^{o}C (ref Figure 10 & 11) no. of damaged regions was higher when contrasted from (20µm),

porous appeared at (5µm). Fine structures were seen in test covered at 200°C (ref. Figure 12 & 13); while test covered at 300°C had edge split structures.

Cells were connected on the surface of Al-Cu-N gatherings with good morphology. Also, cells on Al-Cu-N movies demonstrated more filopodia (appears as a red bolt) at high amplification. In connection with the after-effects of fluorescence recolouring, it can be reasoned that the Al-Cu-N film gave a remarkable condition to the connection and spreading. Numerous examinations have detailed that surface unpleasantness essentially influenced the cell reaction to the material, and the surface harshness affects cell adhesion. Combined with the consequence of AFM pictures, the Al-Cu-N film critically expanded the harshness of the substrates, which can be the reason behind the better cell attachment on Al-Cu-N gathering.

The thickness estimations of 100 ° c, 200 ° c, 300 ° c samples are 229.765 nm, 234.895 nm 260.995 nm respectively. By looking at qualities at various temperatures we observed that the thickness estimation of the 300 ° c the example is higher than the 100 ° c and 200 ° c sample. By this, we can infer that the unpleasantness esteem will increment as the temperature increments

Scanning Electro Microscope (SEM)

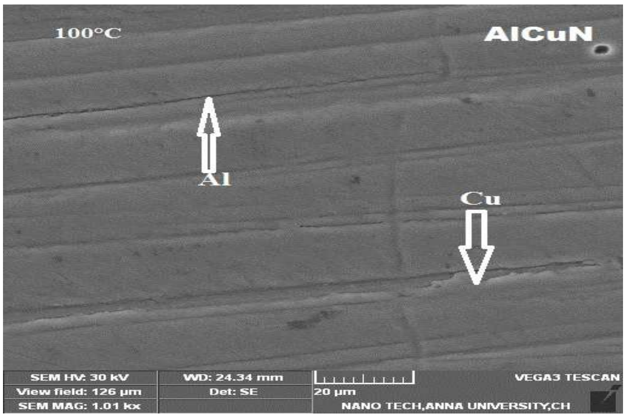

Figure 14: Al-Cu-N Thin Films Deposited on High Speed Substrates at Temperature 100°C (20µm)

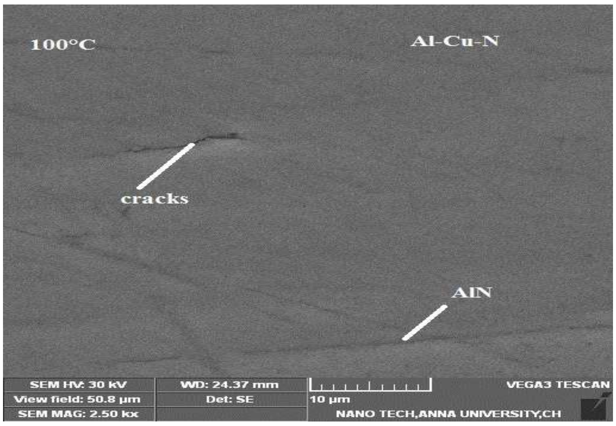

Figure 15: Al-Cu-N Thin Films Deposited on High Speed Substrates at Temperature 100°C (10µm)

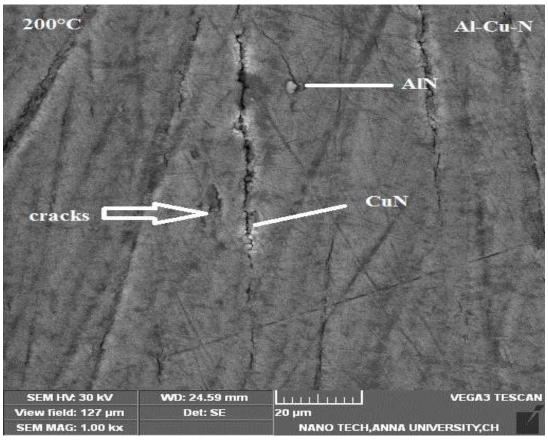

Figure 16: Al-Cu-N Thin Films Deposited on High Speed Substrates at Temperature 200°C (20µm)

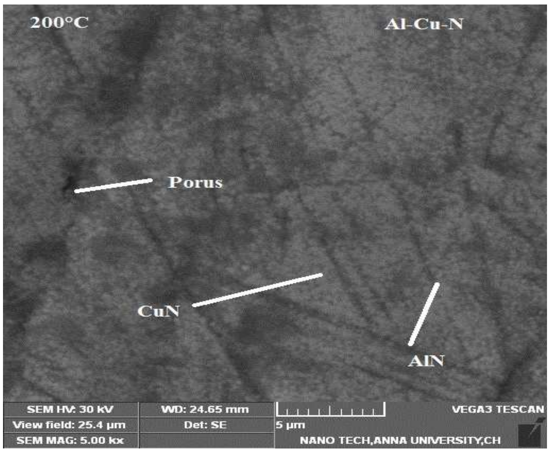

Figure 17: Al-Cu-N Thin Films Deposited on High Speed Substrates at Temperature 200°C (5µm)

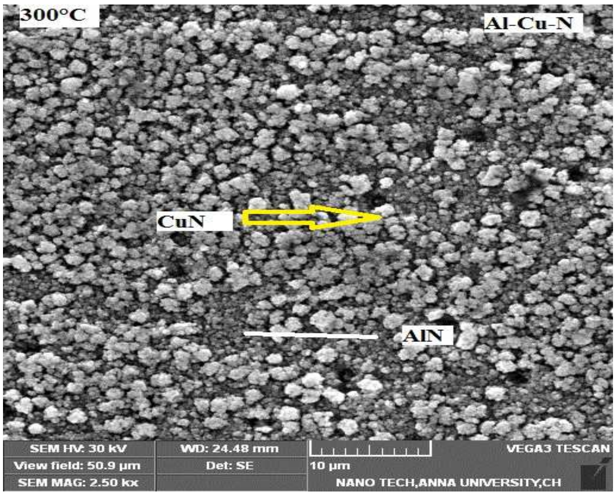

Figure 18: Al-Cu-N Thin Films Deposited on High Speed Substrates at Temperature 300°C (10µm)

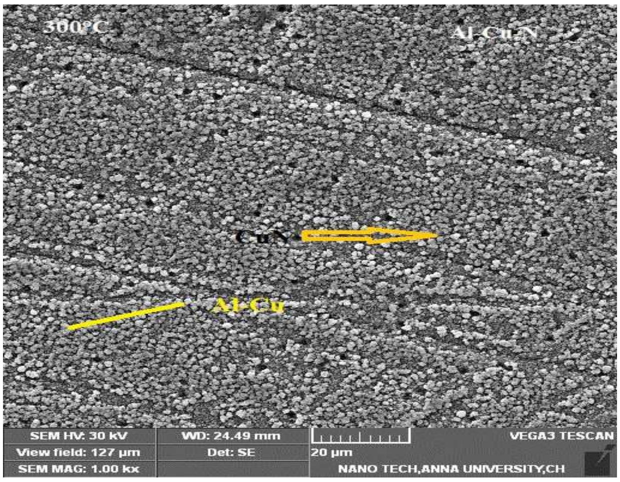

Figure 19: Al-Cu-N Thin Films Deposited on High Speed Substrates at Temperature 300°C (20µm)

Cross-sectional pictures of Al-Cu-N coatings saved under various temperatures appeared in figure 14 to19. From figure 14 & 15 we watched cracks apart at 10µm scale. Under different amplifications and scales, we observed unpredictable structures on the 100^{o} C sample. For tests covered at 200^{o} C (Figure 16&17) no. of damaged regions was higher when contrasted from (20µm), porous appeared at (5µm). Fine structures were seen in test covered at 200^{o}C (Figure 18 & 19); while test covered at 300^{o} C had edge split structures.

Cells were connected on the surface of Al-Cu-N gatherings with good morphology. Also, cells on Al-Cu-N movies demonstrated more filopodia (appears as a red bolt) at high amplification. In connection with the after-effects of fluorescence recolouring, it can be reasoned that the Al-Cu-N film gave a remarkable condition to the connection and spreading. Numerous examinations have detailed that surface unpleasantness essentially influenced the cell reaction to the material, and the surface harshness affects cell adhesion. Combined with the consequence of AFM pictures, the Al-Cu-N film critically expanded the harshness of the substrates, which can be the reason behind the better cell attachment on Al-Cu-N gathering.

Thickness Measurement

Table 4: Thickness Values

S. No	Temperature (°C)	Thickness values(nm)
1	100	229.765
2	200	234.895
3	300	260.995

The thickness estimations of 100^{0} C, 200^{0}C, 300^{0} C samples are 229.765 nm, 234.895 nm 260.995 nm respectively. By looking at qualities at various temperatures we observed that the thickness estimation of the 300^{0}C the example is higher than the 100^{0} C and 200^{0}c sample. By this, we can infer that the unpleasantness esteem will increment as the temperature increments.

Micro Hardness

Characterization of mechanical properties of the films was performed using Vickers hardness. The hardness H v 50 gms was carried for temperature 100 ° c, & 200 °c and 300 °c (10g, 25g, 50g) respectively from 0.025 nm. At each

point Al–Cu–N films sputtered under various deposition conditions demonstrated that the Al–Cu–N films with high hardness H up to ~ 23 GPa, high proportion H/E ≥ 0.1, high flexible recuperation We ≥ 60%, compressive full scale pressure (σ b 0) and Cu substance up to ~12 at.% can be shaped if an adequate vitality Ei is conveyed to the developing film by bombarding ions and quick neutrals.

CORROSION TEST

Corrosion Test with Salt Spray

Corrosion test was performed at various parameters like 5.2% of sodium chloride focus and the temperature in the chamber was 34.0-35.10c. The Ph of the salt arrangement was 6.7 and pneumatic stress was 15 psi and the accumulation of arrangement every hour was 1.3ml. The technique for cleaning of the sample before stacking is done by cleaning delicately and then preceding stacking and thereafter washed tenderly in clean running water to expel testing salt stores from their surfaces and afterwards dried promptly. After this, no consumption happened until 12 hours. Hence the introduction timeframe expanded to 24 hours then red erosion was observed.

Table 5: Corrosion (Salt Spray) Test Observations for 100^{0}c, 200^{0}c

Sl.No	Time	Observation
1	At 24 Hrs	No corrosion
2	At 48 Hrs	Red corrosion observed

CORROSION TEST WITH HUMIDITY

Material

Round coin machined out of high-speed steel was covered with Al-Cu-N covering by R.F/D.C magnetron sputtering process. This substrate was subjected to a salt shower in a chamber mist test according to ASTM benchmarks. All the surface of the covered example was subjected to Salt splash mist consumption test according to ASTM B-117 of salt shower chamber. The example was kept in holders with recognizable proof Nos.

In this sort of corrosion, the humidity was noted as 98% by hygrometer amid the test. The temperature of the test showed 330c-350c. The weight of air for atomizing was 2-3 bars consistently by a weight controller. The piece of the salt answer for 1 litre of arrangement is 5% of sodium chloride and 1% of magnesium chloride De-ionized water is 94% PH of the arrangement which is kept at 7.5 by the expansion of cradle arrangement. Estimation of Ph is done once in 8 hours. Arrangement of stacking of sample tied with plastic wires and hung in the holders was subjected to cleaning with non-watery solvable material which isn't assaulting base material steel with Tantalum nitride covering. The soluble cleaning was done just on the surfaces of the coin on both the sides

Results

Table 6: Corrosion (Fog with Humidity) Test Observations for 300^{0}c

Sample ID	Initial Weight in gm	Final Weight in gm (After 24 hrs.)	Increase in Weight In gm	% Increase in weight
Al-Cu-N	11.424	11.409	0.015	0.131%

CONCLUSIONS

The experiments described in this article show that AlCuN films are new hard and super hard nanocomposites consisting of hard (nc-AlN x) and soft Cu phase up to a hardness of x 48 GPa. The presence of Al in nanocomposites leads to new properties of AlCuN materials. AlCuN easily forms a disordered structure characterized by a broad low-intensity X-ray reflection. The material consists of small (10 nm) grains. The AlCuN film with (less than 10 nm) small grains has a value of 0.5 GPa and exhibits low macro stress. Also, Young's modulus at a given hardness is low. ZrCuN nanocomposites offer greater resistance to plastic deformation of AlCuN materials. Its findings: (i) reduce small (10 nm) particles. Macro stress of less than 0.5 GPa. (Ii) The elements forming hard nitride makes it possible to change the E of the material at a given hardness. Time Control of the mechanical behaviour of nanocomposites is of great scientific and practical importance.

The main purpose of the presented work was to prove that Al-Cu-N nitride film can have three functions simultaneously: (1) to kill bacterium on their surface, (2) to resist mechanical damages and (3) to exhibit increased resistance to cracking throughout bending.

When Al-Cu-N films are sputtered under different deposition conditions, the hardness of the Al-Cu-N films is up to 23 GPa. The ratio H / E 0.1 0.1, the elastic recovery rate at 60%, sufficient macro pressure are supplied for growing film by bombardment with ions and fast neutral energy E i, so σ b 0)-. The Cu contents of up to about 12 atomic % can be formed. (I) -7 to 12 at. A Cu content in the considerable % range was found sufficient to effectively kill E. coli bacteria, and (ii) a combination of high hardness H, high ratio H / E / ≦ 0 High has the elastic recovery and has 60 % of the compressive stress σ leading to (a) cracks during bending and (b) improved resistance of the foil against mechanical damages. These facts clearly show that it is trifunctional: -antibacterial/flexible/ protective. Al-Cu-N films exist and can be made by magnetron sputtering. These films kill E. coli both in sunlight and in the dark.

REFERENCES

1. *R. K. Choudhary, P. Mishra, A. Biswas, and A. C. Bidaye" Structural and Optical Properties of Aluminum Nitride Thin Films Deposited by Pulsed DC Magnetron Sputtering" Volume 2013, Article ID 759462, 5 pages, Hindawi Publishing Corporation.*
2. *Shakil Khan, Muhammad Shahid, A.Mahmood "Texture of the nano-crystalline AlN thin films and the growth conditions in DC magnetron sputtering" Progress in Natural Science: Materials International 25(2015)282–290.*
3. *Neelam Kumari, Ashwini K. Singh and P.K. Barhai" Study of Properties of AlN Thin Films Deposited by Reactive Magnetron Sputtering" Int. J. Thin Fil. Sci. Tec. 3, No. 2, 43–49 (2014).*
4. *Nirun Witit-anun,Jakrapong Kaewkhao and Surasing Chaiyakun "Effect of Sputtering Power on Structural and Optical Properties of AlN Thin Film Deposited by Reactive DC Sputtering Technique" Advanced Materials Research Vol. 770 (2013) pp 177–180.*
5. *Khaled Hussein Metwaly, Ali Hassan Saudy, Farouk Fahmy El-Akshar" Properties of Copper nitride thin films deposited using a pulsed hollow cathode discharge" Volume 1–2 Number 3, Journal of Advances in Physics.*
6. *J. Kiwi, S. Rtimi and C. Pulgarin" Cu, Cu/TiO2 thin films sputtered by up to date methods on non-thermal thin resistant substrates leading to bacterial inactivation" FORMATEX 2013, Microbial pathogens and strategies for combating them: science, technology and education.*

7. *S. Veprek, P. Nesladek, A. Niederhofer, H. Mannling, M. Jılek,in: A. Kumar, Y.-W. Chung, J.J. Moore, J.E. Smugeresky Eds. , Surface Engineering: Science and Technology I, The Minerals, Metals & Materials Society, (1999) 219 .*

8. *P.H. Mayrhofer, C. Mitterer, High-T Properties of Nano composite TiB N and TiB C Coatings, ICMCTF-2000, SanDiego USA, 2000 .*

9. *J. Musil, F. Regent, J. Vac. Sci. Technol. A 16 6 1998 3301.*

10. *J. Musil, P. Zeman, H. Hruby, P.H. Mayrhofer, Surf. Coat. ´ Ž.Technol. 120–121 (1999) 179.*

11. *J. Musil, H. Polakova, Surf. Coat. Technol. 127 (2000) 99.*

12. *J. Musil, H. Hruby, Thin Solid Films 365 (2000) 104.*

13. *J. Musil, P. Karvankova, Surf. Coat. Technol. 139 (2001) 101.*

14. *G.G. Stoney, Proc. R. Soc. Lond. Ser. A 82 (1909) 172.*

15. *Kashyap, R. A. M. G. O. P. A. L., & Gautam, P. R. A. T. I. M. A. (2013). Microarray image segmentation using improved GOGAC method. Science and Engineering (IJCSE), 2(4), 67-74.*

16. *T.Y. Tsui, G.M. Pharr, W.C. Oliver et al., Mater. Res. Soc Symp. Proc. 383 (1995) 447.*

17. *Neelam Kumari, Ashwini K. Singh and P.K. Barhai" Study of Properties of AlN Thin Films Deposited by Reactive Magnetron Sputtering" Int. J. Thin Fil. Sci. Tec. 3, No. 2, 43-49 (2014).*

18. *Abid Iqbal and Faisal Mohd-Yasin" Reactive Sputtering of Aluminum Nitride (002) Thin Films for Piezoelectric Applications" Sensors 2018, 18, 1797.*

19. *Guangan Zhang, Zhibin Lu, Jibin Pu, Guizhi Wu, and Kaiyuan Wang" Structure and Thermal Stability of Copper Nitride Thin Films" Hindawi Publishing Corporation, Journal of Materials Science, Volume 2013, Article ID 725975, 6 pages.*

20. *Ramanjaneyulu, K. S., & Padma, K. (2014). Voltage Profile Enhancement in a Power System Based on SVC Control Strategy Using PSIM Software. IMPACT: International Journal of Research in Engineering and Technology, 2 (2): 213, 222.*

21. *A. Hojabri, N. Haghighian, K. Yasserian, M. Ghoranneviss" The effect of nitrogen plasma on copper thin film deposited by DC magnetron sputtering" Materials Science and Engineering 12 (2010) 012004.*

22. *R. Hariharan, R. Raja, Somu.vasu, "Mechanical and tribological behaviour of thin TaN coating produced on AISI1018 substrate by DC magnetron sputtering" IJRTE, Vol. 7,issue-6S2, April 2019.*